


BRIEF COMMUNICATION

Homozygous variant in *COQ7* causes autosomal recessive hereditary spastic paraplegia

Yusen Qiu^{1,2}, Ying Xiong¹, Lulu Wang¹, Min Zhu^{1,2}, Dandan Tan^{1,2} & Daojun Hong^{1,2,3,4} ¹Department of Neurology, The First Affiliated Hospital of Nanchang University, Nanchang, China²Rare Disease Center, The First Affiliated Hospital of Nanchang University, Nanchang, China³Institute of Neurology, Jiangxi Academy of Clinical Medical Science, The First Affiliated Hospital, Jiangxi Medical College, Nanchang University, Nanchang, China⁴Key Laboratory of Rare Neurological Diseases of Jiangxi Provincial Health Commission, Jiangxi Medical College, Nanchang University, Nanchang, China

Correspondence

Daojun Hong, Department of Neurology, The First Affiliated Hospital of Nanchang University, 17# Yongwazheng Street, Nanchang, China. Tel: +86 791 8869 2511; Fax: +86 791 8869 2511; E-mail: hongdaojun@hotmail.com

Received: 4 January 2024; Revised: 14 February 2024; Accepted: 24 February 2024

Annals of Clinical and Translational Neurology 2024; 11(4): 1067–1074

doi: 10.1002/acn3.52037

Introduction

Hereditary spastic paraplegia (HSP) is a group of genetically heterogeneous diseases primarily characterized by a progressive spastic gait. The length-dependent degeneration of the corticospinal tracts is a pathological hallmark of HSP, resulting in bilateral limb spasticity, hyperreflexia, and extensor plantar responses.¹ HSPs can be classified into pure and complicated forms, depending on whether they coexist with other symptoms such as epilepsy, ataxia, and peripheral neuropathy. Several genes associated with HSP are identified annually, and a total of 91 subtypes of HSP have been identified to date (<https://neuromuscular.wustl.edu/spinal/fsp.html>). Nevertheless, a significant number of patients with spastic paraplegia (SPG) remain genetically unresolved.²

Coenzyme Q₁₀ (CoQ10), also known as ubiquinone, functions as an electron carrier in the mitochondrial respiratory chain.³ It shuttles electrons from Complex I or Complex II to Complex III in the inner mitochondrial membrane.⁴ Primary CoQ10 deficiency is caused by mutations in the genes that are responsible for its

Abstract

Biallelic mutations in the coenzyme Q7 (*COQ7*) encoding gene were recently identified as a genetic cause of distal hereditary motor neuropathy. Here, we explored the clinical, electrophysiological, pathological, and genetic characteristics of a Chinese patient with spastic paraplegia associated with recessive variants in *COQ7*. This patient carried a novel c.322C>A (p.Pro108Thr) homozygous variant. Sural biopsy revealed mild mixed axonal and demyelinating degeneration. Immunoblotting showed a significant decrease in the *COQ7* protein level in the patient's fibroblasts. This study confirmed that *COQ7* variant as a genetic cause of HSP, and further extended spastic paraplegia to the phenotypic spectrum of *COQ7*-related disorders.

intracellular biosynthesis. Recent studies have found that patients with biallelic mutations in *COQ7*, a component of CoQ10 biosynthesis, can present with symptoms resembling HSP or HSP-like.^{5–8} However, there are no entries in the OMIM or neuromuscular website indicating that *COQ7* variants can cause HSP. In this study, we report a case of juvenile-onset HSP, accompanied by epilepsy, distal amyotrophy, and weakness, which is associated with a homozygous variant (c.322C>A, p.Pro108Thr) in the *COQ7* gene.

Materials and Methods

This study was approved by the Ethics Committee of the First Affiliated Hospital of Nanchang University [SJNKHDJ20221213160659]. Written informed consent was obtained from the participants.

DNA was extracted from the patient's peripheral blood leukocytes. The causative gene in the index patient (IV:2) was explored using a whole exome sequence (WES). Sanger sequencing with specific primers was performed to confirm the *COQ7* variant in the parents and available

sibling. Homozygous regions were analyzed using Automap software (<https://automap.iob.ch/>).

Sural nerve biopsy was conducted in the index patient. The nerve was fixed in 4% formaldehyde, paraffin-embedded, cut into 4 μ m sections, and stained by hematoxylin–eosin (HE) staining. Immunostaining with neurofilament (NF) and myelin basic protein (MBP) antibodies was conducted. The rest of the nerve specimen was fixed in 3% glutaraldehyde and embedded in Epon 812. Semithin sections were stained with toluidine blue.

Total cell lysates were subjected to sodium dodecyl sulfate–polyacrylamide gel electrophoresis and immunoblotting. Antibodies were targeted against COQ7 (Proteintech) and tubulin (Proteintech).

Results

The proband (Fig. 1A) was a 34-year-old female patient from a consanguineous family. At the age of 11, she began to feel tightness in her lower limbs, which led to frequent falls and difficulty in walking long distances. At that same year, she experienced several generalized tonic–clonic seizures. Five years later, she noticed muscle weakness and wasting in her lower limbs, which resulted in the spraining and stubbing of her toes while walking on flat roads. Recently, she had occasionally experienced urinary incontinence when she was in urgent need of urination. Her stiffness in her lower limbs had worsened. The muscle weakness and wasting in the lower limbs were more pronounced with mild muscle wasting observed in the hands (Fig. 1B). The physical examination revealed decreased muscle strength in the distal limbs and pyramidal tract signs (Table S1). There were no sensory deficits, signs of ataxia or cognitive impairments. There were no abnormal clinical symptoms or signs observed in the parents and siblings of the patient.

Nerve conduction studies revealed a reduction in compound motor action potential in multiple motor nerves, with a more pronounced severity in the lower limbs compared to the upper limbs. However, the nerve conduction velocity and latency remained within the normal range. The sensory nerves were intact (Table S2). The needle electromyography showed a chronic active neurogenic pattern in the quadriceps femoris and anterior tibialis muscles. At this time, the electroencephalogram was

found to be normal. During the hearing, fundus, and cardiac examinations, no abnormalities were detected. The cerebral MRI demonstrated a normal structure, whereas the spinal MRI revealed a mild atrophy of the thoracic spinal cord (Fig. 1C).

By analyzing the patient's WES data, we identified a novel COQ7 homozygous variant (c.322C>A, p.Pro108Thr, NM_016138.5). This variant is not found in multiple human genome databases, including 1000G, ExAC, and gnomAD. The mutant is highly conserved among species (Fig. 1D) and predicted to be harmful or probably pathogenic using MutationTaster, SIFT, Polyphen2, and CADD software. The Sanger sequence indicated a co-segregation in the family. Using Automap software (<https://automap.iob.ch/>), we found that a total homozygous regions were ~171.46 Mb in the patient, with the variant situated within the largest homozygous region, spanning ~23.09 Mb (chr16:5533549–28620242) (Fig. 1E).

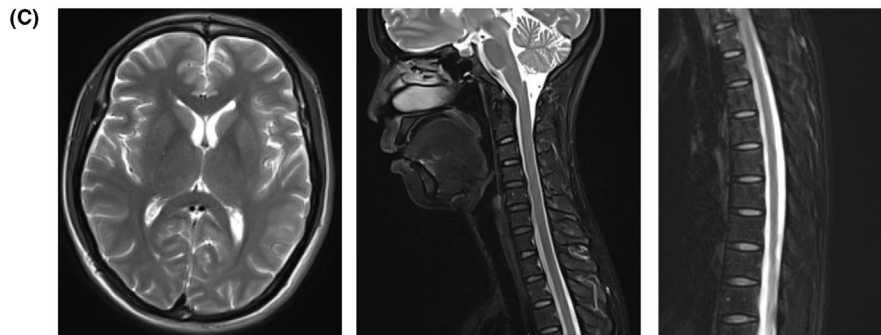
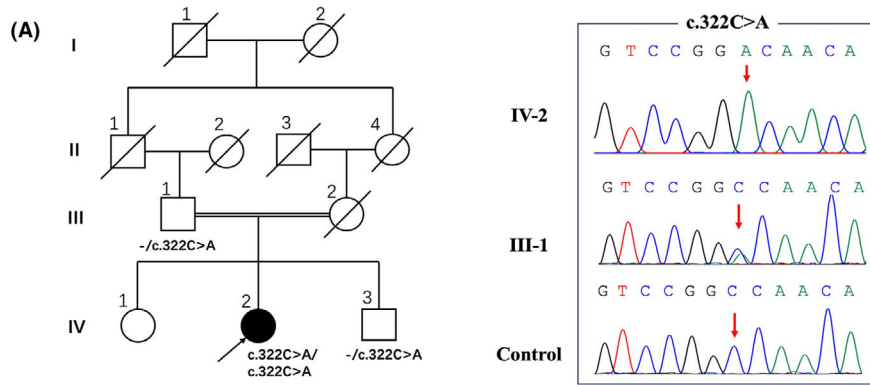
Pathologically, no abnormalities of the sural nerve were observed on HE staining (Fig. 2A). Immunohistochemical staining of MBP antibody showed the normal structure of myelinated fibers (Fig. 2B). However, the toluidine blue staining revealed a slight decrease in the density of myelinated nerve fibers, accompanied by a few thin myelinated fibers (Fig. 2C), indicating a mild mixed axonal and demyelinating degeneration of sensory nerves. Electron microscopy demonstrated the presence of thin myelinated fibers, while the density of unmyelinated axons was slightly decreased with the formation of atypical collagen pockets (Fig. 2D).

In order to evaluate the pathogenic role of the variant, we detected the expression level of COQ7 protein from the patient's skin fibroblasts. Western blot analysis showed that compared with the normal control, the COQ7 protein level in the patient's skin fibroblasts was significantly decreased, which suggested that this homozygous variant resulted in protein instability, leading to loss-of-function mechanism (Fig. 2E).

Discussion

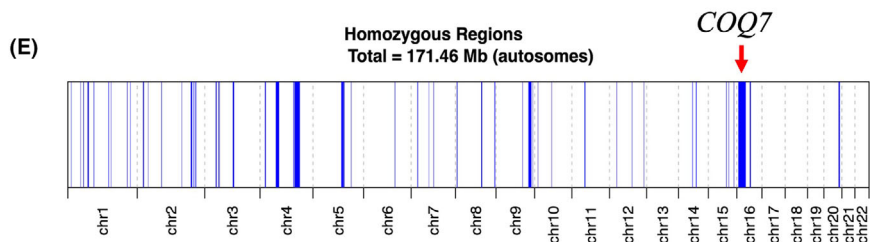
COQ7 variants are the genetic cause of a group of neurodevelopmental disorders. To date, a total of 34 patients with COQ7 mutations have been reported.^{7–9} Despite

Figure 1. Clinical features of the index patient with COQ7 homozygous variant. (A) Left: Pedigree diagram of this family. Right: Sanger sequencing chromatograms showed homozygous and heterozygous c.322C>A variants in this family. (B) Left: Muscle wasting of the distal lower limbs. Right: Muscle wasting of distal upper limbs. (C) Magnetic resonance T2-weighted images of the index patient's brain, cervical spinal cord, and thoracic spinal cord. (D) The conservation of proline at 108 residue in different species. (E) Chromosomal homozygous region of the patient. The red arrow indicates the region where the COQ7 is located.



(D) AA position 108

HUMAN	F	N	E	L	M	V	T	F	R	V	R	P	T	V	L	M	P	L	W	N
RAT	F	N	E	L	M	V	A	F	R	V	R	P	T	V	L	M	P	L	W	N
MOUSE	F	N	E	L	M	I	A	F	R	V	R	P	T	V	L	M	P	L	W	N
YEAST	F	N	N	L	Q	L	K	R	R	V	R	P	S	L	L	T	P	L	W	K
BOVIN	F	N	E	L	M	V	A	F	R	V	R	P	T	V	L	M	P	F	W	N
SCHPO	F	D	N	Y	V	L	K	N	R	V	R	P	T	F	L	R	P	F	W	D
CAEEL	M	E	R	L	A	A	K	H	N	V	P	H	T	V	F	S	P	V	F	S



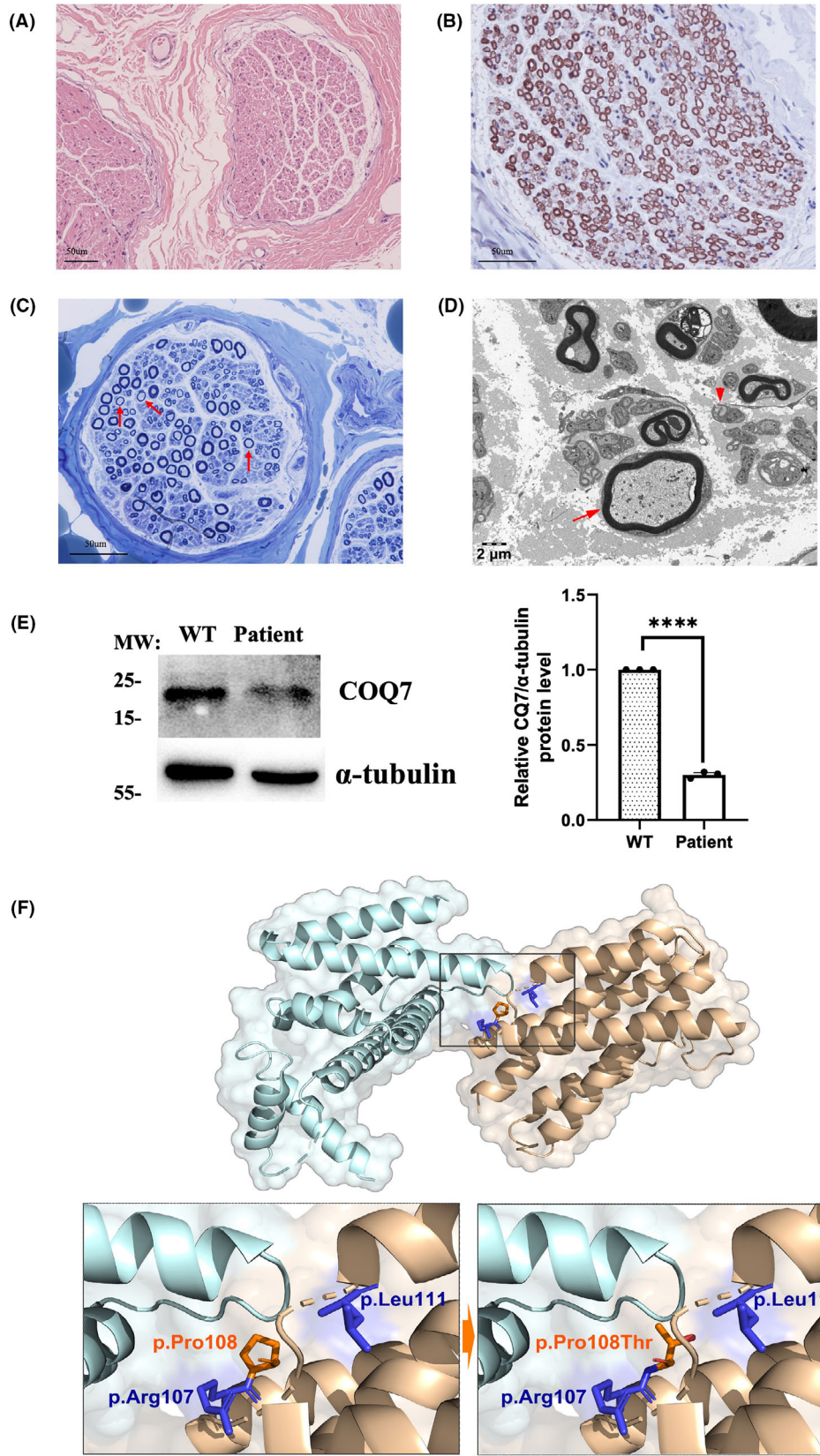


Figure 2. Neuropathological and molecular changes in patient and predicted structure changes of COQ7 protein. (A) HE staining revealed the normal structure of sural nerve. (B) Immunohistochemical staining of MBP antibody revealed the normal structure of myelinated fibers in sural nerve. (C) Toluidine blue staining revealed a mild reduction in the density of myelinated nerve fibers and a few thin myelinated fibers (Red arrow). (D) Electron microscopy revealed thin myelinated fibers (Red arrow) and a mild reduction of the density of unmyelinated axons with atypical collagen pockets (Red arrowhead). (E) Western blot analysis of COQ7 protein level was significantly decreased compared with the normal control in skin fibroblasts. (F) Structure of the COQ7:COQ9 dipolymer (PDB ID 7SSP) and mapped by PyMOL. Details for p.Pro108Thr mutant interfering the COQ7:COQ9 interaction.

incomplete clinical data for some patients, the most common clinical manifestations included muscle weakness (27/29), muscle atrophy (26/29), increased knee reflexes (22/32), and increased muscle tone of lower limbs (11/21). Our patient presented with juvenile-onset HSP, characterized by spastic gait, limb rigidity, hyperreflexia, patellar clonus, extensor plantar responses, and bladder dysfunction. Additionally, she was accompanied by epilepsy and distal motor neuropathy (dHMN), which can be categorized as a complex HSP.

Recently, several articles have reported that biallelic mutations in the *COQ7* gene caused dHMN with or without upper motor neuron signs. The axonal degeneration of motor nerves and corticospinal tracts was a continuous spectrum of axonopathy, so it was reasonable for some patients with *COQ7*-related disorder to exhibit predominant dHMN accompanied by upper motor neuron signs. Vice versa, it was also possible for some patients could exhibit a dominance of HSP along with dHMN. Additionally, at least 16 subtypes of complex HSP could also exhibit spasticity combined with motor neuropathy, such as SPG17 and SPG38,^{10,11} among others. Their clinical manifestations were very similar to those of patients with *COQ7* variants. Therefore, the clinical phenotypes of *COQ7*-related disorders can be divided into three distinct subgroups (Table 1). The first was a developmental encephalomyopathy (5/34). The second group exhibited milder forms of peripheral neuropathy with or without upper motor neuron signs (24/34). The final group comprised patients with either pure or complex HSP (5/34).

Patients with *COQ7* mutations primarily exhibited axonopathy in the nervous system; however, there were no autopsy reports for these individuals. This study provided the first case (albeit of a sensory nerve) of neuropathological findings, characterized by decreased axonal density, thin myelin sheath of large myelinated fibers, and degeneration of unmyelinated fibers. Pathologically, we speculated that our patient might eventually develop axonal Charcot-Marie-Tooth (CMT2), despite currently presenting with dHMN at electrophysiological level.

COQ7 plays a key role in the penultimate step of COQ10 biosynthesis. The structure of COQ7 contains six helices ($\alpha 1$ - $\alpha 6$), helices $\alpha 1$, $\alpha 3$, $\alpha 4$, and $\alpha 6$ form a hydrophobic surface and a large hydrophobic channel.¹²

COQ7 binds to COQ9 at this hydrophobic surface to form a complex, the reported mutations associated with HSP phenotype are located on this hydrophobic surface (p.Arg107Trp, p.Pro108Thr, and p.Leu111Pro)^{5,13} (Fig. 2F). We speculated that these mutants near this structure might affect the binding between COQ7 and COQ9, which might potentially modify the clinical manifestations. Mutations in *COQ4*, another gene involved in the biosynthesis of CoQ10, have been reported to cause HSP and epilepsy. COQ4 protein levels in fibroblasts derived from patients with *COQ4*-related HSP were reduced, but only slightly reducing CoQ10 levels. A similar metabolic pattern had also been observed in a case with *COQ7* p.Leu111Pro variant. In this study, we also observed that COQ7 protein levels in fibroblasts derived from patient with the *COQ7*-related HSP were significantly decreased. Although the p.Pro108Thr variant (1995683) had been reported as uncertain significance on ClinVar, considering the preliminary functional studies, this missense variant could be classified as likely pathogenic. It can be speculated that the milder clinical phenotype may be associated with a mild reduction rather than a severe reduction in CoQ10. Given that neurons were highly sensitive to energy restrictions, the mitochondrial dysfunction caused by the slight reduction in CoQ10 might be more susceptible to affecting neurons.

In summary, while only one family was included in this study, the patient exhibited a typical phenotype of complex HSP and was associated with a novel homozygous variant in *COQ7*, which expanded the spectrum of pathogenic variants and clinical phenotypes of *COQ7*-related disorders. The *COQ7* gene should be included in the genetic workflow for the diagnosis of HSP.

Acknowledgment

We thank the patients and their families for their participation in this study. This work was supported by the National Natural Science Foundation of China (Grants 82160252 and 82271439), Natural Science Foundation of Jiangxi province (20224ACB206015), and Double thousand talents program of Jiangxi province (jxsq2019101021).

Table 1. The summary of reported patients with COQ7 mutations.

Phenotype	Variants	Origin	Gender	Family	Age at onset (years)	Manifestations	Reference
Encephalomyopathy							
Encephalomyopathy	c.599_600delins/c.319C>T	China	Male	Consanguineous	After birth	Fatal developmental encephalomyopathy	Kwong, et al. (2019)
Encephalomyopathy	Homozygous c.422T>A	Syrian	Male	Consanguineous	After birth	Progressive encephaloneuro-nephro-cardiopathy	Freyer et al. (2015)
Encephalomyopathy	c.308C>T/c.332T>C	Canada	Female	Consanguineous	2	Global developmental delay with spastic paraplegia	Wang et al. (2017)
Encephalomyopathy	Homozygous c.161G>A	Turkey	Female	Nonconsanguineous	5	Language and motor developmental delay	Wang et al. (2022)
Encephalomyopathy	c.446A>G/c.161G>A	European	Male	Nonconsanguineous	After birth	Developmental encephalomyopathy	Parith et al. (2023)
Peripheral neuropathy							
dHMN with UMN signs	Homozygous c.3G>T	Portugal	Male	Nonconsanguineous	12	Progressive atrophy and weakness of the distal muscles	Jacquier et al. (2023)
dHMN with UMN signs	Homozygous c.3G>T	Portugal	Female	Nonconsanguineous	9	Progressive atrophy and weakness of the distal muscles	Jacquier et al. (2023)
dHMN	Homozygous c.3G>T	Portugal	Male	Nonconsanguineous	10	Progressive atrophy and weakness of the distal muscles	Jacquier et al. (2023)
dHMN	c.253-2A>T/c.467T>A	China	Male	Nonconsanguineous	14	Progressive atrophy and weakness of the distal muscles	Liu et al. (2023)
dHMN	c.160C>T/c.467T>G	China	Male	Nonconsanguineous	15	Progressive atrophy and weakness of the distal muscles	Liu et al. (2023)
dHMN	Homozygous c.1A>G	Syria	Male	Consanguineous	10	Progressive atrophy and weakness of the distal muscles	Smith et al. (2023)
dHMN	Homozygous c.1A>G	Syria	Female	Consanguineous	10	Progressive atrophy and weakness of the distal muscles	Smith et al. (2023)
dHMN	Homozygous c.1A>G	Syria	Male	Consanguineous	10	Progressive atrophy and weakness of the distal muscles	Smith et al. (2023)
dHMN	c.197T>A/c.446A>G	USA	Male	Nonconsanguineous	Mid-teens	Walking and running difficulties	Rebello et al. (2023)
dHMN	c.197T>A/c.446A>G	USA	Male	Nonconsanguineous	Childhood	Never able to run, walking difficulties	Rebello et al. (2023)
dHMN	c.197T>A/c.319C>T	Brazil	Male	Nonconsanguineous	<10	Walking and running difficulties	Rebello et al. (2023)
dHMN with UMN signs	Homozygous c.161G>A	Brazil	Female	Nonconsanguineous	3	Walking and running difficulties	Rebello et al. (2023)

(Continued)

Table 1 Continued.

Phenotype	Variants	Origin	Gender	Family	Age at onset (years)	Manifestations	Reference
dHMN with UMN signs	Homozygous c.3G>T	Brazil	Female	Nonconsanguineous	5	Walking and running difficulties	Rebello et al. (2023)
dHMN with UMN signs	Homozygous c.3G>T	Brazil	Female	Nonconsanguineous	10	Walking and running difficulties	Rebello et al. (2023)
dHMN	Homozygous c.3G>T	Brazil	Female	Nonconsanguineous	1	Walking and running difficulties	Rebello et al. (2023)
dHMN	Homozygous c.3G>T	Brazil	Female	Consanguineous	School age	Walking difficulties	Rebello et al. (2023)
dHMN	Homozygous c.3G>T	Brazil	Male	Consanguineous	4	Walking and running difficulties	Rebello et al. (2023)
dHMN	Homozygous c.3G>T	Brazil	Female	Consanguineous	10	Walking and running difficulties	Rebello et al. (2023)
CMT2	Homozygous c.319C>T	Wales	Male	Consanguineous	8–10	Walking difficulties	Rebello et al. (2023)
CMT2	c.467T>G/ c.599_600delins	China	Male	Nonconsanguineous	6	Progressive atrophy and weakness of the distal muscles	Zhang et al. (2023)
CMT	c.446A>G/c.3G>T	NA	Female	NA	12	Progressive weakness of lower limbs	Parith et al. (2023)
CMT	Homozygous c.161G>A	Brazil	Female	NA	3	Equine posturing and pes cavus deformity	Parith et al. (2023)
CMT	c.197T>A/ c.446A>G	Netherlands	NA	Nonconsanguineous	NA	Axonal neuropathy, mild neurodegenerative disorder	Tom et al. (2017)
CMT	c.197T>A/ c.446A>G	Netherlands	NA	Nonconsanguineous	NA	Axonal neuropathy, mild neurodegenerative disorder	Tom et al. (2017)
HSP							
HSP-like	Homozygous c.332T>C	Iran	Male	Consanguineous	1	Moderate progressive spastic paraparesis	Sadr et al. (2023)
HSP-like	Homozygous c.161G>A	Brazil	Female	Consanguineous	3	Progressive spastic paraplegia	Parith et al. (2023)
HSP-like	Homozygous c.3G>T	Brazil	Female	Consanguineous	5	Progressive spastic paraplegia	Parith et al. (2023)
HSP-like	c.308C>T/ c.332T>C	Iran	Female	Consanguineous	2	Moderate to severe progressive spastic paraplegia	Hashemi et al. (2021)
HSP-like	Homozygous c.322C>A	China	Female	Consanguineous	11	HSP with epilepsy, distal amyotrophy, and weakness	This study

Abbreviations: CMT, Charcot-Marie-Tooth; dHMN, distal hereditary motor neuropathy; HSP, hereditary spastic paraplegia; NA, not available; UMN, upper motor neuron.

Author Contributions

D.H. and Q.Y. contributed to the conception and design of the study; Y.X. and M.Z. contributed to the acquisition and analysis of data; L.W. and D.T. contributed to drafting the text and preparing the figures.

Funding Information

This work was supported by the National Natural Science Foundation of China (Grants 82160252 and 82271439), Natural Science Foundation of Jiangxi province (20224ACB206015), and Double thousand talents program of Jiangxi province (jxsq2019101021).

Conflict of Interest Statement

The authors have no conflicts of interest to declare.

References

1. Shribman S, Reid E, Crosby AH, Houlden H, Warner TT. Hereditary spastic paraplegia: from diagnosis to emerging therapeutic approaches. *Lancet Neurol.* 2019;18(12):1136-1146.
2. Schüle R, Wiethoff S, Martus P, et al. Hereditary spastic paraplegia: Clinicogenetic lessons from 608 patients. *Ann Neurol.* 2016;79(4):646-658.
3. Staiano C, García-Corzo L, Mantle D, et al. Biosynthesis, deficiency, and supplementation of coenzyme Q. *Antioxidants (Basel).* 2023;12(7):1469.
4. Guerra RM, Pagliarini DJ. Coenzyme Q biochemistry and biosynthesis. *Trends Biochem Sci.* 2023;48(5):463-476.
5. Hashemi SS, Zare-Abdollahi D, Bakhshandeh MK, et al. Clinical spectrum in multiple families with primary COQ(10) deficiency. *Am J Med Genet A.* 2021;185(2):440-452.
6. Liu XX, Wang N, Chen YK, et al. Biallelic variants in the COQ7 gene cause distal hereditary motor neuropathy in two Chinese families. *Brain.* 2023;146(5):e27-e30.
7. Zhang XY, Dong HL, Wu ZY. Axonal Charcot-Marie-tooth disease due to COQ7 mutation: expanding the genetic and clinical spectrum. *Brain.* 2023;146:e117-e119.
8. Rebelo AP, Tomaselli PJ, Medina J, et al. Biallelic variants in COQ7 cause distal hereditary motor neuropathy with upper motor neuron signs. *Brain.* 2023;146(10):4191-4199.
9. Wongkittichote P, Duque Lasio ML, Magistrati M, et al. Phenotypic, molecular, and functional characterization of COQ7-related primary CoQ(10) deficiency: hypomorphic variants and two distinct disease entities. *Mol Genet Metab.* 2023;139(4):107630.
10. Windpassinger C, Auer-Grumbach M, Irobi J, et al. Heterozygous missense mutations in BSCL2 are associated with distal hereditary motor neuropathy and silver syndrome. *Nat Genet.* 2004;36(3):271-276.
11. Kropatsch R, Schmidt HM, Buttkeireit P, Epplen JT, Hoffjan S. BICD2 mutational analysis in hereditary spastic paraplegia and hereditary motor and sensory neuropathy. *Muscle Nerve.* 2019;59(4):484-486.
12. Manicki M, Aydin H, Abriata LA, et al. Structure and functionality of a multimeric human COQ7:COQ9 complex. *Mol Cell.* 2022;82(22):4307-4323.e4310.
13. Sadr Z, Zare-Abdollahi D, Rohani M, Alavi A. A founder mutation in COQ7, p.(Leu111Pro), causes pure hereditary spastic paraplegia (HSP) in the Iranian population. *Neurol Sci.* 2023;44(7):2599-2602.

Supporting Information

Additional supporting information may be found online in the Supporting Information section at the end of the article.

Table S1.